crystallization communications

Crystallization and preliminary X-ray diffraction analysis of transaldolase from *Thermoplasma acidophilum*

Anja Lehwess-Litzmann,[a,b] **Piotr Neumann,**[a,b] **Ralph Golbik,**[b] **Christoph Parthier**[b] **and Kai Tittmann**[a,b]*

[a]Göttinger Zentrum für Molekulare Biowissenschaften, Georg-August-Universität Göttingen, Ernst-Caspari-Haus, Justus-von-Liebig-Weg 11, D-37077 Göttingen, Germany, and [b]Naturwissenschaftliche Fakultät I, Institut für Biochemie und Biotechnologie, Martin-Luther-Universität Halle-Wittenberg, Kurt-Mothes-Strasse 3, D-06120 Halle, Germany

Correspondence e-mail: ktittma@gwdg.de

The metabolic enzyme transaldolase from *Thermoplasma acidophilum* was recombinantly expressed in *Escherichia coli* and could be crystallized in two polymorphic forms. Crystals were grown by the hanging-drop vapour-diffusion method using PEG 6000 as precipitant. Native data sets for crystal forms 1 and 2 were collected in-house to resolutions of 3.0 and 2.7 Å, respectively. Crystal form 1 belonged to the orthorhombic space group $C222_1$ with five monomers per asymmetric unit and crystal form 2 belonged to the monoclinic space group $P2_1$ with ten monomers per asymmetric unit.

1. Introduction

Transaldolase (TA) is a ubiquitous enzyme of carbon metabolism that catalyzes the reversible transfer of a three-carbon dihydroxyacetone unit between sugar phosphates as part of the nonoxidative part of the pentose phosphate pathway (Samland & Sprenger, 2009). In the cellular context, it catalyzes the interconversion of the ketose substrates fructose 6-phosphate (F6P) and sedoheptulose 7-phosphate (S7P) in an equilibrium reaction with the aldose phosphates erythrose 4-phosphate (E4P) and glyceraldehyde 3-phosphate (G3P) as alternative acceptor substrates,

fructose 6-phosphate + erythrose 4-phosphate

$$\longleftrightarrow \text{seduheptulose 7-phosphate} + \text{glyceraldehyde 3-phosphate.} \quad (1)$$
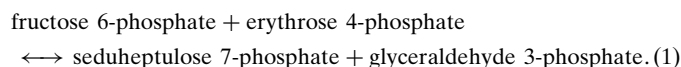
TA does not contain a cofactor but utilizes an active-centre lysine that forms Schiff-base adducts with donor ketose substrates in a multistep reaction sequence involving carbinolamine-type, iminium-type and enamine-type intermediates. Structural analysis of TAs from different organisms by X-ray diffraction revealed that all hitherto characterized TA proteins fold into an $(\alpha/\beta)_8$-barrel (TIM barrel) consisting of alternating α-helices and β-strands in a doughnut-shaped structure, the central core of which is constituted of eight parallel β-strands (Jia, Huang *et al.*, 1996; Thorell *et al.*, 2000). Despite the overall conserved subunit topology and fold, different quaternary assemblies are observed for TAs from different domains of life (Samland & Sprenger, 2009). While TAs from bacteria and eukarya form homodimers, the archaeal enzymes exist as homodecamers made up of two pentameric discs (a dimer of two pentamers) in a face-to-face orientation.

A molecular reaction mechanism for TA has been proposed on the basis of mutagenesis studies and structural analysis of a borohydride-reduced dihydroxyacetone Schiff-base adduct trapped at the active site of TA from *Escherichia coli* (Jia *et al.*, 1997; Schörken *et al.*, 2001). The steady-state kinetic data and structural information implicated two conserved acidic residues, a Glu and an Asp, as functioning as general acid/base catalysts at different stages of the reaction cycle. The conserved Glu has been proposed to first activate the essential lysine *via* a bridging catalytic water and then to facilitate dehydration of the transiently formed carbinolamine intermediate. Breakdown of the scissile C3—C4 bond of the Schiff base thus formed is believed to be initiated by ionization of the C4 hydroxyl group catalyzed by the conserved Asp residue. However, this functional assignment needs to be confirmed by structural analysis of genuine reaction intermediates trapped in the active site of a TA.
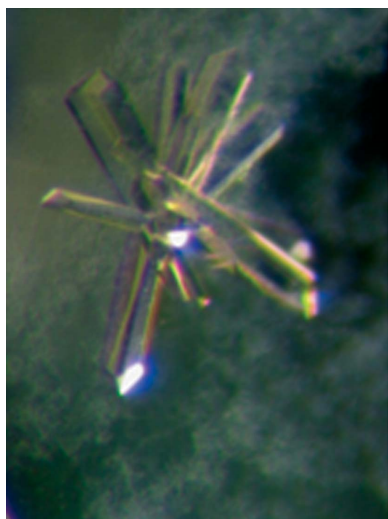
Here, we report the crystallization and preliminary X-ray diffraction analysis of TA from *Thermoplasma acidophilum* (*Tac*TA) as part of a study towards understanding the molecular reaction mechanism of TA by structural analysis of authentic on-pathway intermediates.

2. Materials and methods

2.1. Cloning of *Ta*0616, protein expression and purification

An operon encoding transketolase I (*Ta*0618), transketolase II (*Ta*0617) and transaldolase (*Ta*0616) from *T. acidophilum* was amplified from chromosomal DNA of *T. acidophilum* using PCR. The whole operon was then cloned into pET28a vector (Novagen) using *Nde*I and *Hin*dIII restriction sites and appropriate primers (MWG Biotech). A double stop codon was inserted at the end of gene *Ta*0616 encoding *Tac*TA (residues 1–223) to prevent expression of the C-terminal His tag. The correctness of the sequence was confirmed by complete sequencing of the gene.

*Tac*TA was heterologously expressed in *E. coli* BL21 Star (DE3) (Invitrogen). Cells were grown for 14–18 h at 310 K after induction of gene expression with 0.5 mM IPTG. The protein was initially enriched by fractional ammonium sulfate precipitation, in which the protein precipitated in the fraction containing 50–80%(w/v) ammonium sulfate. This fraction was desalted by exhaustive dialysis against 20 mM Tris–HCl pH 7.5 at 279 K and was then further purified using a Fractogel EMD TMAE (S) (Merck KgaA, Germany) anion-exchange step (elution buffer: 20 mM Tris pH 7.5 supplemented with 1 M NaCl) and subsequent heat precipitation (20 min at 333 K). The homogeneity was judged by SDS–PAGE analysis. Finally, the buffer was exchanged to 20 mM glycylglycine pH 7.5 and the protein was stored at 273–279 K until use.

2.2. Steady-state kinetic analysis

Transaldolase activity (conversion of the donor F6P and the acceptor E4P into the products G3P and S7P) was analyzed in a coupled spectrophotometric steady-state assay using the auxiliary enzymes triosephosphate isomerase (TIM) and *sn*-glycerol-3-phosphate:NAD$^+$ 2-oxidoreductase (G3PDH) to detect the formation of G3P, which is derived from the cleavage of F6P. The concomitant

oxidation of NADH was followed spectrophotometrically at 340 nm in 20 mM glycylglycine pH 7.5 supplemented with 50 U ml^{-1} TIM, 5 U ml^{-1} G3PDH and varying concentrations of F6P (up to 15 mM) and E4P (up to 2 mM) at 303 K. Potential F6P or fructose 1,6-bis-phosphate (FBP) aldolase activity was tested with the same assay but using F6P or FBP as the sole substrate (in the absence of any acceptor substrate).

2.3. Crystallization and data collection

Crystals of *Tac*TA were grown by the hanging-drop vapour-diffusion method at 291 K using a modification of the protocol that was established for the crystallization of TA from *E. coli* (Jia, Lindqvist *et al.*, 1996). A 3 μl droplet of 16 mg ml^{-1} *Tac*TA in a two-component buffer (6 mM Tris and 14 mM glycylglycine pH 7.5) was mixed with 3 μl reservoir solution consisting of 0.1 M sodium citrate pH 4, 10%(w/v) PEG 6000 and 25%(v/v) glycerol and equilibrated against 500 μl reservoir solution. The pH of the resulting crystallization mixture was determined to be 4.5.

Crystals of *Tac*TA were mounted in cryoloops (Hampton Research, USA), flash-cooled by direct immersion in liquid nitrogen and placed on the goniometer head. Diffraction data for both crystal forms were collected in-house with an R-AXIS IV^{++} imaging-plate system (Rigaku–MSC, Japan) using Cu $K\alpha$ radiation with a wavelength of 1.5418 Å generated by a rotating-anode generator (Rigaku MicroMax-007). Data sets were collected under cryogenic conditions at 100 K (XSTREAM2000, Rigaku–MSC, Japan). Data sets were processed and scaled using *XDS* (Kabsch, 2010).

3. Results and discussion

*Tac*TA could be recombinantly produced in *E. coli* strain BL21 (DE3) Star, for which the highest expression yields were obtained amongst a set of different tested strains. Starting from 10 g cell material, a total of 15–20 mg protein could be purified to homogeneity by fractional salt precipitation, anion-exchange chromatography and heat precipitation. Purified *Tac*TA exhibited a single band at 26 kDa on SDS–PAGE, which is in reasonable agreement with the calculated molecular mass of 24 437 Da. The enzyme consists of 223 amino-acid residues and thus belongs to the transaldolase-like
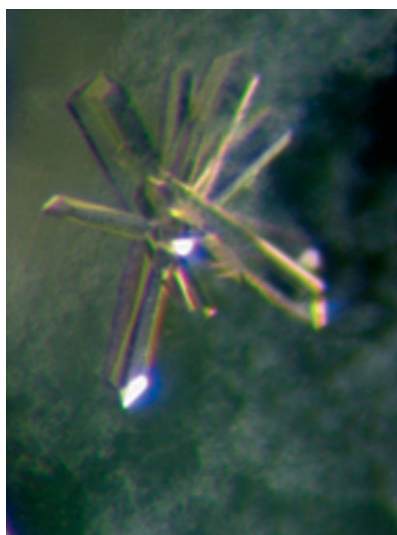

Figure 1
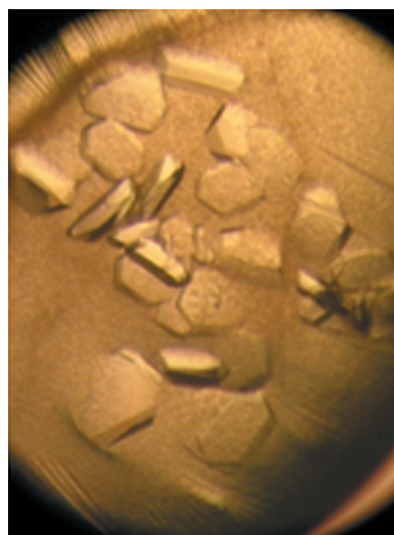Representative crystal (0.6 × 0.1 × 0.1 mm) of *Tac*TA in the orthorhombic space group $C222_1$.

Figure 2
Representative crystal (0.4 × 0.4 × 0.1 mm) of *Tac*TA in the monoclinic space group $P2_1$.

crystallization communications

	Crystal form 1	Crystal form 2
Space group	$C222_1$	$P2_1$
Unit-cell parameters (Å, °)	$a = 147.10$, $b = 171.30$, $c = 98.90$, $\alpha = \beta = \gamma = 90.0$	$a = 98.98$, $b = 129.17$, $c = 100.10$, $\alpha = \gamma = 90.0$, $\beta = 108.2$
Resolution range (Å)	29.63–3.00 (3.10–3.00)	29.40–2.70 (2.80–2.70)
Mosaicity (°)	0.39	0.23
No. of observations	138527 (13021)	474815 (36419)
No. of unique reflections	24858 (2303)	65081 (6176)
$\langle I/\sigma(I)\rangle$	20.8 (4.2)	21.0 (5.3)
Completeness (%)	97.9 (99.8)	98.9 (91.3)
Multiplicity	5.6 (5.6)	7.3 (5.9)
R_{merge}† (%)	7.8 (44.9)	8.1 (33.5)
R_{meas}‡ (%)	8.6 (49.5)	8.7 (36.8)
B factor from Wilson plot (Å²)	54.5	49.3
Matthews coefficient (Å³ Da⁻¹)	2.63	2.56
Monomers in asymmetric unit	5	10

† $R_{\mathrm{merge}} = \sum_{hkl}\sum_i |I_i(hkl) - \langle I(hkl)\rangle|/\sum_{hkl}\sum_i I_i(hkl)$; ‡ $R_{\mathrm{meas}} = \sum_{hkl}[N/(N-1)]^{1/2}$ $\times \sum_i |I_i(hkl) - \langle I(hkl)\rangle|/\sum_{hkl}\sum_i I_i(hkl)$, where $I_i(hkl)$ is the intensity of the ith observation of reflection hkl and $\langle I(hkl)\rangle$ is the mean value of $I_i(hkl)$ for all measurements; N is the multiplicity.

proteins, which are approximately 100 residues shorter in length than the classical transaldolases (Samland & Sprenger, 2009). Steady-state kinetic analysis confirmed that *Tac*TA exhibits transaldolase activity, as predicted from sequence similarity to TAs from other organisms, with a k_{cat} of 16.61 ± 1.11 s⁻¹ (303 K, pH 7.5) at saturating concentrations of the substrates F6P and E4P. In contrast, no F6P or fructose 1,6-bisphosphate aldolase activity could be detected.

Two polymorphic crystal forms of *Tac*TA were obtained under identical chemical conditions at 291 K. It turned out that the temperature conditions of crystallization setup prior to crystallization were important in determining which crystal form was preferentially grown. When crystallization setup was carried out at 303 K, *Tac*TA crystallized in form 1 with approximate crystal dimensions of 0.6 × 0.1 × 0.1 mm (Fig. 1). In contrast, a second crystal form (form 2) with dimensions of 0.4 × 0.4 × 0.1 mm (Fig. 2) was obtained when crystallization was set up at 291 K. Occasionally, crystals of both forms grew in the same drop. However, when crystals of form 2 appeared first it was rarely observed that the other crystal form grew in the same drop.

Native data sets from crystal forms 1 and 2 were collected in-house under cryogenic conditions to resolutions of 3.0 and 2.7 Å, respectively (Table 1). The space group of form 1 was identified as the orthorhombic space group $C222_1$, while form 2 belonged to the monoclinic space group $P2_1$. Initial molecular-replacement phasing using the structure of TA from *Thermus thermophilus* HB8 (PDB

entry 1wx0; Y. Asada & N. Kunishima, unpublished work) as a search model with *Phaser* (Winn *et al.*, 2011) was successful and revealed the presence of either five (form 1) or ten (form 2) monomers in the asymmetric unit. The Matthews coefficients were 2.63 Å³ Da⁻¹ (form 1) and 2.56 Å³ Da⁻¹ (form 2), indicating a similar solvent content of ~52% for both crystal forms, which falls within the typical range for protein crystals. Initial trials showed that both crystal forms could withstand soaking with substrate solution.

We are now aiming at collecting data sets at higher resolution using synchrotron radiation and additionally solving the structures of reaction intermediates after soaking *Tac*TA crystals with different physiological substrates in order to obtain further insights into the enzymatic reaction mechanism. In this context, we also wish to analyze whether or not similar catalytic principles govern the processing of the sugar substrates and derived intermediates to those that have recently been proposed for transketolase (Asztalos *et al.*, 2007; Tittmann & Wille, 2009). As opposed to TA, transketolase transfers two-carbon rather than three-carbon units and contains the bioorganic cofactor thiamine diphosphate. Since the molecular origins of the different bond-fission specificity in the two enzymes are not understood, a comparative structural analysis of reaction intermediates will provide insight.

References

Asztalos, P., Parthier, C., Golbik, R., Kleinschmidt, M., Hübner, G., Weiss, M. S., Friedemann, R., Wille, G. & Tittmann, K. (2007). *Biochemistry*, **46**, 12037–12052.
Jia, J., Huang, W., Schörken, U., Sahm, H., Sprenger, G. A., Lindqvist, Y. & Schneider, G. (1996). *Structure*, **4**, 715–724.
Jia, J., Lindqvist, Y., Schneider, G., Schörken, U., Sahm, H. & Sprenger, G. A. (1996). *Acta Cryst.* D**52**, 192–193.
Jia, J., Schörken, U., Lindqvist, Y., Sprenger, G. A. & Schneider, G. (1997). *Protein Sci.* **6**, 119–124.
Kabsch, W. (2010). *Acta Cryst.* D**66**, 125–132.
Samland, A. K. & Sprenger, G. A. (2009). *Int. J. Biochem. Cell Biol.* **41**, 1482–1494.
Schörken, U., Thorell, S., Schürmann, M., Jia, J., Sprenger, G. A. & Schneider, G. (2001). *Eur. J. Biochem.* **268**, 2408–2415.
Thorell, S., Gergely, P., Banki, K., Perl, A. & Schneider, G. (2000). *FEBS Lett.* **475**, 205–208.
Tittmann, K. & Wille, G. (2009). *J. Mol. Cat. B Enzym.* **61**, 93–99.
Winn, M. D. *et al.* (2011). *Acta Cryst.* D**67**, 235–242.